The Cryosphere Discuss., 4, 1243–1276, 2010
www.the-cryosphere-discuss.net/4/1243/2010/
doi:10.5194/tcd-4-1243-2010

The Cryosphere Discussions

An energy-conserving model of freezing variably-saturated soil

M. Dall'Amico[1,*], S. Endrizzi[2], S. Gruber[3], and R. Rigon[1]

[1]Department of Civil and Environmental Engineering, University of Trento, Trento, Italy
[2]Environment Canada – National Hydrology Research Centre, Saskatoon, Saskatchewan, Canada
[3]Department of Geography, University of Zurich, Winterthurerstrasse 190 Zurich, Switzerland
[*]now at: Mountain-eering srl, Via Siemens 19 Bolzano, Italy

Received: 29 June 2010 – Accepted: 9 July 2010 – Published: 11 August 2010

Correspondence to: M. Dall'Amico (matteo@mountain-eering.com)

Published by Copernicus Publications on behalf of the European Geosciences Union.

Abstract

In this paper we provide a method for solving the energy equation in freezing soil. The solver is linked with the solution of Richards equation, and therefore able to approximate water movement near the liquid-solid phase transition. The equations show non-linear characteristics causing oscillatory behavior in the solution close to the phase transition, when normal methods of iterative integration, as Newton or Picard, are used. Thus, a globally convergent Newton method has been implemented to achieve convergence. The method is tested by comparison with an analytical solution to the Stefan problem and by comparison with experimental data derived from literature.

1 Introduction

The analysis of freezing/thawing processes and phenomena in the ground are important for hydrological and other land surface and climate model simulations (e.g., Viterbo et al., 1999; Smirnova et al., 2000). For example, comparisons of results from the Project for Intercomparison of Land Surface Parameterization Schemes Phase 2(d) [PILPS 2(d)] have shown that the models with an explicit frozen soil scheme provide more realistic soil temperature simulation during winter than those without (Luo et al., 2003). Freezing soil models may be divided into three categories: *empirical and semiempirical*, *analytical*, and *numerical physically-based* (Zhang et al., 2008). Empirical and semiempirical algorithms relate ground thawing-freezing depth to some aspect of surface forcing by one or more experimentally established coefficients (e.g., Anisimov et al., 2002). Analytical algorithms are specific solutions to heat conduction problems under certain assumptions. The most widely applied analytical solution is Stefan's formulation, which simulates the freezing/thawing front using accumulated ground surface degree-days (either a freezing or thawing index) (Lunardini, 1981). Numerical physically-based algorithms simulate ground freezing by numerically solving the complete energy equation and in natural conditions are expected to provide the

TCD
4, 1243–1276, 2010

best accuracy in simulating ground thawing and freezing (Zhang et al., 2008). However, the treatment of latent heat is not an easy task because it is confined to a narrow range near the melting point, and thus represents a discontinuity that may create numerical oscillations (Hansson et al., 2004). Numerical models usually treat the latent heat term using one of these approaches: (i) the pure conduction heat equation is first solved, and then the soil temperature is readjusted by the ratio of liquid and solid water given by energy conservation during phase change (Shoop and Bigl, 1997); (ii) the latent heat term is related to temperature and unfrozen water content by an apparent heat capacity formulation (Williams and Smith, 1989). The objective of this paper is to describe a new formulation for a energy conserving freezing soil algorithm based on the apparent heat capacity method which allows to cope with the high non-linearities introduced by the latent heat term. The algorithm is tested against the analytical solution of unilateral freezing of a semi-infinite region given by Neumann, and the experimental results published by Hansson et al. (2004).

2 Freezing-soil models

One of the first attempts to include soil freeze-thaw into a numerical model is the work of Nakano and Brown (1971) who have assumed the advance of the freezing front as a moving boundary condition. They apply the analytical solution of Carslaw and Jaeger (1959) to a soil of a given porosity, and introduce the effect of an artificial freezing zone of finite width between the frozen and the unfrozen parts, in order to avoid the problem of shock wave propagation in the transition between the frozen and thawed state typical of the classical "freezing front" assumption. No water flow, i.e. no mass balance equation, is taken into account and the energy balance is expressed through the apparent heat capacity formulation as proposed by Lukyanov and Golovko (1957). Harlan (1973) is probably the first to attempt to solve coupled mass and energy balance equations for the freezing soil by making an analogy between the mechanism of water transport in partially frozen soils and those in unsaturated soils. He solves the

TCD
4, 1243–1276, 2010

system on a homogeneous rigid porous medium through a fully implicit finite difference scheme, where the unknowns are temperature and soil water potential; phase change in the water balance appears in the source/sink term. He also uses the apparent heat capacity formulation in the energy balance. The results show that the freezing process induces the movement of both heat and mass from warm to cold regions, causing the moisture content in the unfrozen soil zone to decrease sharply towards the freezing front. Soil texture and initial moisture conditions seem to be crucial in affecting the availability and mobility of water. Fuchs et al. (1978) develop a theory of soil freezing applicable to unsaturated conditions with solute presence in the soil. They consider that solutes tend to depress the freezing point temperature and modify the relationship between temperature, moisture content and apparent thermal properties of the soil. Phase change is taken into account in the apparent heat capacity formulation, and the water flow contribution is accounted for in the apparent thermal conductivity, thus the simultaneous heat and water transport equations result in a merged single differential equation for heat. Jame and Norum (1980) further develop the model of Harlan (1973) and highlight that the effect of mass transfer on the thermal state of soil is an important factor to be considered. Newman and Wilson (1997) propose a theoretical formulation for unsaturated soils using soil-freezing and soil-water characteristic curve data to combine the heat and mass transfer relationships into a single equation for freezing or frozen regions of the soil. Christoffersen and Tulaczyk (2003) have constructed a high-resolution numerical model of heat, water, and solute flows in sub-ice stream till subjected to basal freeze-on. They propose a formulation of the equilibrium relation without assuming zero ice pressure through the full version of the Clapeyron equation, which enable them to model segregation ice onto the freezing interface and so develop stratified basal ice layers. Hansson et al. (2004) introduced a new method for coupled heat transport and variably saturated water flow using the Richards' equation. They account for water flow due to gravity, pressure gradient and temperature gradient, both for liquid and vapor phase. McKenzie et al. (2007) proposed the freezing module of SUTRA for saturated conditions. Daanen et al. (2007) developed a 3-D model of cou-

TCD
4, 1243–1276, 2010

pled energy and Richards equation to analyze the effects that lead to the formation of nonsorted circles, en example of a relatively stable patterned-ground system. Their model is very similar to Hansson et al. (2004) but it differs in the linkage between ice content and temperature. Watanabe (2008) also uses a similar model to Hansson et al. (2004) and reproduces directional freezing experiments on silty soil and compares this with experimental data. Based on these studies, some important aspects in freezing soil algorithms may be highlighted:

1. All authors use the same closure relationship between pressure and temperature in the form of a generalized Clapeyron equation. However, after the first attempt of Loch (1978), to our knowledge this equation has never been fully derived from a thermodynamical point of view leaving some doubt on its limitations.

2. All authors, sometimes explicitly, sometimes implicitly, utilize the "freezing=drying" assumption as suggested by Miller (1965). On the one hand this speculation simplifies the modeling, as it allows to use the same relationships used for unsaturated soils to freezing soils. On the other hand, however, it has profound consequences for the pressures for the water and the ice phases and, therefore, requires a careful analysis in order to understand the type of processes (e.g. frost heave) that can be dealt with.

3. Often, the soil saturation levels the models are dealing with are not specified. Sometimes the pressure-temperature relationships are given for a fully saturated soil, sometimes for a dry soil, leaving doubt about the details of the hypothesis.

4. The energy equation with freezing soil in the above considered literature is always written in a non-conservative form.

TCD
4, 1243–1276, 2010

3 Governing equations

When water and ice coexist in the soil, according to the simplest view of the thermodynamic phenomenon, three main equations must be used to describe their evolution: (1) an equation that relates the pressures of water and ice with their volumetric content, (2) the energy budget and (3) the mass budget.

3.1 Water and ice content

The soil is composed of soil particles (subscript sp), liquid water (subscript w), ice (subscript i) and air (Fig. 1). We define the total volumetric water content Θ (–) as the sum of the liquid θ_w (–) and the solid (ice) θ_i (–) water content, according to the respective densities:

$$\Theta := \theta_w + \frac{\rho_i}{\rho_w}\theta_i \tag{1}$$

where ρ_w and ρ_i ($kg\,m^{-3}$) are the densities of water and ice. The total volumetric water content is subject to the following limitations given by the residual water content θ_r and the soil porosity θ_s:

$$0 \le \theta_r \le \Theta \le \theta_s \le 1 \tag{2}$$

In the soil volume, ice and water are present, each with its own characteristic tension and pressure. According to the "freezing=drying" assumption (Miller, 1965; Spaans and Baker, 1996), the ice pressure may be set to null and so the generalized Clausius-Clapeyron equation becomes:

$$L_f \frac{dT}{T} = g\,d\psi \tag{3}$$

where L_f is the latent heat of fusion ($J\,kg^{-1}$), T (K) is the temperature, g ($m\,s^{-2}$) is the acceleration due to gravity and ψ (m) is the pressure head of water. This equation

TCD
4, 1243–1276, 2010

states that the variation of water pressure during phase change is just dependent on temperature. If the soil is unsaturated the water pressure ψ_{w0} is negative, due to the surface tension of the water-air interface. This fact changes the water melting temperature T^*, which becomes lower than the melting temperature T_m=273.15 K at atmospheric pressure p_a. Putting p_a=0 as a reference, it is possible to determine T^* by integrating the above equation and solving against temperature:

$$\int_{T_m}^{T^*} L_f \frac{dT}{T} = \int_0^{\psi_{w0}} g d\psi \tag{4}$$

and so, assuming that:

$$\int_{T_m}^{T^*} L_f \frac{dT}{T} = \ln\left(\frac{T^*}{T_m}\right) \approx \frac{T^* - T_m}{T_m} \tag{5}$$

one obtains:

$$T^* = T_m + \frac{gT_m}{L_f}\psi_{w0} - \frac{gT_m}{L_f}\psi_{w0} \cdot H(\psi_{w0}) \tag{6}$$

where $H(\ )$ is the Heaviside function. This equation states that when the initial water pressure in the soil volume $\psi_{w0} \geq 0$ (i.e. the soil is saturated and no water-air interfaces are present), the freezing temperature is $T^*=T_m$. When the soil is unsaturated ($\psi_{w0}<0$), then the melting temperature falls and results $T^*<T_m$. Equation (6) improves the findings of Eq. (3) of Zhang et al. (2007) as it gives the validity field of water pressure. Zhang et al. (2007) state that the freezing point depression is given by $\psi=(L_f T)/g(T_0)$ where 273.16 K is the freezing point of free water, however, this is only true at the triple point and variable with atmospheric pressure.

TCD
4, 1243–1276, 2010

The pressure of liquid water may be determined by integrating Eq. (3) from T^* to T in temperature and from ψ_{w0} to ψ in pressure:

$$\int_{T^*}^{T} L_f \frac{dT}{T} = \int_{\psi_{w0}}^{\psi} g \, d\psi \tag{7}$$

and consequently the new liquid water pressure becomes:

$$\psi(T) = \psi_{w0} \cdot H(T - T^*) + \frac{L_f}{gT^*}(T - T^*) \cdot H(T^* - T) \tag{8}$$

The above equation states that the liquid water pressure is equal to the depression ψ_{w0} given by the desaturation degree when $T \geq T^*$, and is equal to the freezing depression given by the Clausius-Clapeyron equation when $T < T^*$.

The water content in the soil may be related to the soil pressure head ψ according to the soil water retention curve, e.g., Brooks and Corey (1964), Clapp and Hornberger (1978), Gardner (1958) and Van Genuchten (1980). According to the Van Genuchten (1980) model, the volumetric liquid water content θ_w (–) becomes:

$$\theta_w[\psi(T)] = \theta_r + (\theta_s - \theta_r) \cdot \left\{1 + [-\alpha \, \psi(T)]^n\right\}^{-m} \tag{9}$$

When $\psi = \psi_{w0}$ (i.e. $T \geq T^*$), the liquid water content equals the volumetric total water content Θ present in the volume and dependent on the desaturation level:

$$\Theta = \theta_r + (\theta_s - \theta_r) \cdot \left\{1 + \left[-\alpha \, \psi_{w0}\right]^n\right\}^{-m} \tag{10}$$

Eventually the volumetric ice content θ_i may be derived by Eq. (1):

$$\theta_i = \frac{\rho_w}{\rho_i}[\Theta - \theta_w[\psi(T)]] \tag{11}$$

TCD
4, 1243–1276, 2010

3.2 Mass balance

The variation of liquid water during the time interval dt in the control volume, excluding ice movements, is due to the contemporary action of flow through the boundaries and phase transformation. To simplify the problem, as commonly done in the literature, we assume that the two actions (flux and phase transformation) can be distinguished in time, i.e. in the first $dt/2$ we have the water flux and in the second $dt/2$ we have phase transition. The mass conservation in a soil volume may be written as:

$$\rho_w \frac{\partial \Theta}{\partial t} + \rho_w \nabla \cdot \boldsymbol{J}_w + \rho_w S_w = 0 \tag{12}$$

S_w (s^{-1}) is a sink term due to evapotranspiration and $\boldsymbol{J}_w$ ($m\,s^{-1}$) is the water flux within the soil and follows the Darcy-Buckingham formulation:

$$\boldsymbol{J}_w(\psi) = -\boldsymbol{K}_H \nabla(\psi + z_f) \tag{13}$$

$K_H = K_H(\psi)$ ($m\,s^{-1}$) is the hydraulic conductivity (Mualem, 1976), and z_f (m) is the elevation with respect to a reference and represents the gravitational head. Notice that the ice flux $\boldsymbol{J}_i$ ($m\,s^{-1}$) within the soil is neglected.

The derivative of the total water content $\partial\Theta/\partial t$ may be written as:

$$\rho_w \frac{\partial \Theta}{\partial t} = \rho_i \frac{\partial \theta_i}{\partial t} + \rho_w \frac{\partial \theta_w(\psi)}{\partial t} \tag{14}$$

In this case, during the second $dt/2$, no phase change is occurring and therefore $\partial\theta_i/\partial t \equiv 0$. Eventually the mass balance equation becomes:

$$\frac{\partial \theta_w(\psi)}{\partial t} + \nabla \cdot \boldsymbol{J}_w(\psi) + S_w = 0 \tag{15}$$

TCD
4, 1243–1276, 2010

3.3 Energy balance

The energy conservation in a soil volume V_c may be written as:

$$\frac{\partial U}{\partial t} + \boldsymbol{\nabla} \cdot (\boldsymbol{G} + \boldsymbol{J}) + S_{en} = 0 \quad (16)$$

where the symbol "·" refers to the internal product, the symbol $\boldsymbol{\nabla} = \left(\frac{\partial}{\partial x}; \frac{\partial}{\partial y}; \frac{\partial}{\partial z}\right)$ (m^{-1}) to the gradient operation.

S_{en} $(W\,m^{-3})$ represents a sink term due to energy losses, U $(J\,m^{-3})$ is the volumetric internal energy and $\boldsymbol{G}$ $(W\,m^{-2})$ is the conduction through the volume boundaries. According to the Fourier law, $\boldsymbol{G}$ equals to:

$$\boldsymbol{G} = -\boldsymbol{\lambda}_T(\Theta, T) \cdot \boldsymbol{\nabla} T \quad (17)$$

where λ_T $[W\,m^{-1}\,K^{-1}]$ is the thermal conductivity of the soil matrix that depends on the proportions of ice and water given by the degree of saturation Θ and the temperature T (Johansen, 1975; Farouki, 1981). $\boldsymbol{J}$ $(W\,m^{-2})$ is the advective heat flux by water flow and may be calculated as:

$$\boldsymbol{J} = \rho_w \cdot \boldsymbol{c}_w \boldsymbol{J}_w \cdot T \quad (18)$$

where $\boldsymbol{J}_w$ $(m\,s^{-1})$ is the water flux within the soil (see Eq. 13) and c_w $(J\,kg^{-1}\,K^{-1})$ is the specific thermal capacity of water. In addition to pressure-induced gradients, temperature gradients create a pressure difference and thus water flow between the warmer and colder regions. The flow of water can advect heat.

3.4 The internal energy

The internal energy U of V_c, neglecting the energy of air and excluding the work of volume expansion passing from the liquid to the frozen state, may be calculated as the sum of the internal energy of the soil particles, ice and liquid water:

$$U = U_{sp} + U_i + U_w \quad (19)$$

TCD
4, 1243–1276, 2010

In particular, with regard to a reference temperature $T_{ref}=T_m$, one gets that $T-T_{ref}\equiv T$ (°C). Therefore each of the above terms becomes:

$$\begin{cases} U_{sp}(T) = C_{sp}(1-\theta_s)T \\ U_i(\theta_i,T) = \rho_i\theta_i c_i T \\ U_w(\theta_w,T) = \rho_w\theta_w[L_f + c_w T] \end{cases} \quad (20)$$

where c_i (J kg^{-1} K^{-1}) is the specific thermal capacity of ice and T is from now on to be intended in (°C). Summing the components in Eq. (20) in a more compact term gives:

$$U = C_T \cdot T + \rho_w L_f \theta_w \quad (21)$$

where $C_T := C_{sp}(1-\theta_s)+\rho_i c_i \theta_i + \rho_w c_w \theta_w$ (J m^{-3} K^{-1}) is the total thermal capacity of the soil volume. Deriving Eq. (21) with respect to t one may write:

$$\frac{dU}{dt} = C_T\frac{dT}{dt} + \rho_i c_i \frac{\partial\theta_i}{dt} + \rho_w c_w \frac{\partial\theta_w}{\partial t} + \rho_w L_f \frac{\partial\theta_w}{\partial t} \quad (22)$$

During phase change no water flux is considered (which makes the volume a closed system), and so, for mass conservation:

$$\rho_i \frac{\partial\theta_i}{\partial t} = -\rho_w \frac{\partial\theta_w}{\partial t} \quad (23)$$

The above equation states that the mass of water subject to phase change is equal to the mass of ice subject to phase change. Inserting Eq. (23) in Eq. (22) results in:

$$\frac{dU}{dt} = C_T\frac{dT}{dt} + \rho_w[(c_w - c_i)\cdot T + L_f]\frac{\partial\theta_w}{\partial t} \quad (24)$$

The variation of liquid water content in time may be calculated through the derivative chain rule:

$$\frac{\partial\theta_w[\psi(T)]}{\partial t} = \frac{\partial\theta_w}{\partial\psi}\cdot\frac{\partial\psi}{\partial T}\cdot\frac{dT}{dt} \quad (25)$$

TCD
4, 1243–1276, 2010

The first derivative $\partial\theta_w/\partial\psi := C_H$ (m^{-1}) is defined as the hydraulic capacity, and is the slope of the soil water retention curve. The second derivative $\partial\psi/\partial T$ represents the slope of the Clausius-Clapeyron equation.

Eventually inserting Eq. (25) into Eq. (22) one gets:

$$\frac{dU}{dt} = C_a(T)\frac{dT}{dt} \tag{26}$$

C_a ($J\,m^{-3}\,K^{-1}$) is the so-called apparent heat capacity (Williams and Smith, 1989):

$$C_a = C_T + \rho_w[L_f + (c_w - c_i)T]C_H\frac{L_f}{g\,T_m}H(T^* - T) \tag{27}$$

and is the sum of the sensible heat transmitted to the soil matrix and the latent released by phase change. The apparent heat capacity is a function of the temperature difference $T^* - T$ and is highly non linear near T^*, where it increases by several orders of magnitude and often induces numerical oscillations (Hansson et al., 2004).

4 The decoupled solution

The system of equations to solve is composed of Eqs. (16) and (15) and represents a coupled system as both equation are contemporarily functions of ψ and T. Let us indicate with the superscript n the quantities at the time step n, with $n+1$ the quantities at $t^{n+1} = t^n + \Delta t$ and with $n+1/2$ the quantities at $t^{n+1/2} = t^n + \Delta t/2$. Assuming that the flux and phase transformation can be separated in time, i.e. water flux occurs in the first $\Delta t/2$ and phase transition in the second $\Delta t/2$, the system can be solved in two steps:

1. Solve Eq. (15) to obtain ψ_{w0}^{n+1} (and through Eq. 10 one finds Θ^{n+1}), $\boldsymbol{J}_w$ and the liquid water content $\theta_w^{n+1/2} = \theta_w^n + \Delta\theta_w^{fl}$ (the superscript fl indicates that the quantity

TCD
4, 1243–1276, 2010

is related to the flux process). $\Delta\theta_w^{fl}$ is subject to the following limitation given by volume conservation:

$$\theta_r - \theta_w^n \le \Delta\theta_w^{fl} \le \theta_s - \theta_w^n - \frac{\rho_i}{\rho_w}\theta_i^n \tag{28}$$

2. Solve Eq. (16) to obtain temperature T^{n+1} and the new proportions of ice and water, given, respectively by: $\theta_i^{n+1}=\theta_i^n+\Delta\theta_i^{ph}$ and $\theta_w^{n+1}=\theta_w^{n+1/2}+\Delta\theta_w^{ph}$. One may realize from Eq. (23) that $\rho_w\Delta\theta_w^{ph}+\rho_i\Delta\theta_i^{ph}=0$ and that $\Delta\theta_w^{ph}$ is subject to the following limitation given by total water content conservation:

$$\theta_r - \theta_w^n - \Delta\theta_w^{fl} \le \Delta\theta_w^{ph} \le \frac{\rho_i}{\rho_w}\theta_i^n - \Delta\theta_w^{fl} \tag{29}$$

The details of the numerical procedure may be found in Dall'Amico (2010).

5 A conservative discretization for the energy equation

The 3-D solver for Eq. (15) is implemented in GEOtop (Endrizzi et al., 2010). This paper deals with the peculiarities of Eq. (16).

Let us consider the dependence of water and ice content on T explicit and let us put $Q(T):=G(T)+J(T)$. Equation (16) becomes:

$$\frac{\partial U(T)}{\partial t} + \nabla\cdot\boldsymbol{Q} + S(T) = 0 \tag{30}$$

Integrating the above in the cell l of volume V and neglecting the lateral energy fluxes (e.g., considering just the vertical fluxes) one gets:

$$\frac{\partial U^*}{\partial t} + Q_{l+1/2} - Q_{l-1/2} + S_l^* = 0 \tag{31}$$

TCD
4, 1243–1276, 2010

where the quantities U^* (J) and S^* (W) are to be considered as the integral in the cell:

$$U^*(T)_l := \int_{V_c} U dV = \int_{z_{l-\frac{1}{2}}}^{z_{l+\frac{1}{2}}} dz \int_{\Omega} U \, d\Omega =$$

$$= \int_{z_{l-1/2}}^{z_{l+1/2}} U(T)\Omega dz \tag{32}$$

$$S^*(T)_l := \int_{z_{l-1/2}}^{z_{l+1/2}} S(T)\Omega dz \tag{33}$$

where Ω (m^2) is the area of the volume surface, e.g. of the cell area. Applying the divergence theorem one gets:

$$\int_{V_c} \nabla \cdot \boldsymbol{Q} dV = \int_{\Omega} \boldsymbol{Q} d\Omega = Q^*_{l+1/2} - Q^*_{l-1/2} \tag{34}$$

with:

$$Q^*_{l+\frac{1}{2}} := -\Omega_{l+\frac{1}{2}} \left(\lambda^n_{l+\frac{1}{2}} \frac{T_{l+1} - T_l}{z_{l+1} - z_l} + \frac{\rho_w c_w J_w T_{l+\frac{1}{2}}}{2} \right)^{n+1}$$

$$Q^*_{l-\frac{1}{2}} := -\Omega_{l-\frac{1}{2}} \left(\lambda^n_{l-\frac{1}{2}} \frac{T_l - T_{l-1}}{z_l - z_{l-1}} + \frac{\rho_w c_w J_w T_{l-\frac{1}{2}}}{2} \right)^{n+1} \tag{35}$$

and it is intended that all the quantities are estimated at the $l \pm 1/2$ boundary of the cell of area $\Omega_{l \pm 1/2}$. After discretization, the equation is still exact and no approximation

TCD
4, 1243–1276, 2010

of any of its quantities has been made (the equation is conservative, and preserves internal energy).

The time derivative in Eq. (31) can be estimated, by using a finite difference scheme between t^n and $t^{n+1}=t^n+\Delta t$. If the Crank-Nicholson strategy is used (Crank and Nicolson, 1996), it is:

$$\frac{U_l^*(T^{n+1})-U_l^*(T^n)}{\Delta t}+Q^*_{l+1/2}(T^{n+1})+-Q^*_{l-1/2}(T^{n+1})+S_l^*(T^{n+1})=0 \tag{36}$$

where energy is integrated over the cell volumes. The discretized equation can be written as:

$$R_l(T^{n+1}):=U_l^*(T^{n+1})-U_l^*(T^n)+\Delta t\left[f_l(T^{n+1})\right]=0 \tag{37}$$

where $R_l(T)$ $l=1\ldots, N$ (J) is a component of an array of N functions, said residuals, and where f_l is the sum of the fluxes and the source term at time $n+1$:

$$f_l(T^{n+1}):=Q^*_{l+1/2}(T^{n+1})-Q^*_{l-1/2}(T^{n+1})+S_l^*(T^{n+1}) \tag{38}$$

$R_l(T^{n+1})$ is a non linear function of the temperature in the l-th volume at time t^{n+1}, and finding its zero (for any l) is equivalent to get the time marching of the internal energy. This problem can be solved iteratively through the Newton method (e.g., Kelley, 2003), which consists of approximating the non linear functions as:

$$R_k(T)^{,m+1}\approx R_k^{,m}+J^{,m}_{R_{l,k}}\cdot(T_k^{,m+1}-T_k^{,m})\quad l,k=1,\ldots,N \tag{39}$$

where "$,m$" is the Newton iteration number, $J^{,m}_{R_{l,k}}$ is the Jacobian matrix of $R_k^{,m}$, and the approximate solution is obtained by solving the linear system (40). The Jacobian is

TCD
4, 1243–1276, 2010

defined as:

$$J^{m}_{R_{l,k}} := \left.\frac{\partial R_l}{\partial T_k}\right|^{,m} = \begin{pmatrix} \frac{\partial R_1}{\partial T_1} & \frac{\partial R_1}{\partial T_2} & \cdots & \frac{\partial R_1}{\partial T_N} \\ \frac{\partial R_2}{\partial T_1} & \frac{\partial R_2}{\partial T_2} & \cdots & \frac{\partial R_2}{\partial T_N} \\ \frac{\partial R_l}{\partial T_1} & \frac{\partial R_l}{\partial T_2} & \cdots & \frac{\partial R_l}{\partial T_N} \\ \frac{\partial R_N}{\partial T_1} & \frac{\partial R_N}{\partial T_2} & \cdots & \frac{\partial R_N}{\partial T_N} \end{pmatrix}^{,m} \tag{40}$$

Considering a constant cell area Ω in the same soil column, the above matrix becomes tridiagonal and is composed by:

$$J^{,m}_{R_{l,k}} = \begin{cases} -\Omega\Delta t \left(\frac{\lambda^n_{l-1/2}}{z_l - z_{l-1}} + \frac{1}{2}\rho_{\mathrm{w}}\, c_{\mathrm{w}}\, J_{\mathrm{w}} \right) & k = l-1 \\ C^m_{\mathrm{a}_l} + \Omega\Delta t \left(\frac{\lambda^n_{l-1/2}}{z_l - z_{l-1}} + \frac{\lambda^n_{l+1/2}}{z_{l+1} - z_l} \right) & k = l \\ -\Omega\Delta t \left(\frac{\lambda^n_{l+1/2}}{z_{l+1} - z_l} + \frac{1}{2}\rho_{\mathrm{w}} c_{\mathrm{w}} J_{\mathrm{w}} \right) & k = l+1 \\ 0 & \text{otherwise} \end{cases} \tag{41}$$

where all the symbols are defined in Table A1. At each of the Newton iterations, say m+1, finding the approximate roots means solving a linear system, and therefore, the Newton method transforms the initial non-linear problem into a sequence of linear problems. In the 1-D case the matrix becomes tridiagonal and the system may be solved by the Thomas algorithm. It is important to notice that if the Newton method is solved exactly, energy is preserved. This differentiates the new method from previous work.

5.1 Globally convergent iteration

The Newton method works well if the initial guess of T_0 is close enough to the true solution T. Typically, a region which is well-behaved is first located with some other method, and Newton's method is then used to refine the solution (the root finding),

TCD
4, 1243–1276, 2010

which is already known approximately. It may happen that the residual array of function close to the solution is not convex or concave (always decreasing or increasing with increasing or decreasing derivative, respectively), and the method may pass from T_0 to T_1 without reaching the convergence, as shown in Fig. 2. In the energy equation solution this happens during the phase transition, when temperature passes from positive to negative values or vice-versa. At positive temperatures the heat capacity is $\approx 2\,\mathrm{MJ\,m^{-3}\,K^{-1}}$ and at $-0.1\,^{\circ}\mathrm{C}$ it assumes more or less the same value. All the latent term of the equation, in fact, is comprised in very small temperature intervals, where the peak of the apparent heat capacity is positioned, and may increase of three orders of magnitude depending on the Van Genuchten parameters. Hansson et al. (2004) recommend, in order to converge, to set the value of the heat capacity to its maximum value when passing from positive to negative temperature. However, this precaution is not sufficient as we observed that the Newton scheme was not converging, and, indeed not necessary. A considerable improvement was obtained changing to the so-called *globally convergent Newton scheme*. This is based on the fact that the direction of the tangent given by the Newton scheme is always good in the sense that it points to the direction of decreasing residuals. Yet the final point may be too far from the solution causing the scheme to oscillate. In order to avoid this, the *globally convergent Newton scheme* tests the residual:

$$\text{if} \quad \|\boldsymbol{R}(T)^{,m+1}\| > \|\boldsymbol{R}(T)^{,m}\| \tag{42}$$

$$\text{then} \quad \boldsymbol{T}^{,m+1} \simeq \boldsymbol{T}^{,m} - \boldsymbol{\Delta T} \cdot \delta \tag{43}$$

This test implies that far from the solution the increment is multiplied by a reduction factor δ with $0 \leq \delta \leq 1$ (e.g., Kelley, 2003). If $\delta = 1$ the scheme coincides with the normal Newton-Raphson scheme. This method, together with the maximum heat capacity imposition, allows the scheme to converge. This scheme is also applied by Tomita (2009) to solve surface energy balance equation, when the surface temperature shows oscillations caused by the exclusion or poor consideration of the surface temperature dependence of the turbulent transfer coefcient at the surface.

TCD
4, 1243–1276, 2010

6 Model testing: analytical solution

Our model was compared against the analytical solution of unilateral freezing of a semi-infinite region given by Neumann. The features of this problem are the existence of a moving interface between the two phases, in correspondence of which heat is liberated or absorbed, and the discontinuity on the thermal properties of the two phases (Carslaw and Jaeger, 1959). Nakano and Brown (1971) give the analytical solution for the case of an initially frozen soil. The assumptions are: (1) constant Dirichlet boundary condition at the top, (2) steady heat flow in both the frozen and thawed regions, (3) change of volume negligible, i.e. $\rho_w=\rho_i$ and (4) isothermal phase change at $T=T_m$, i.e. no unfrozen water exists at temperatures less then the melting temperature T_m. In our numerical scheme we have considered a soil with porosity $\theta_s\equiv1$ (i.e. pure water) characterized by a very steep SFCC with no residual water content, approaching a step function. Assuming a SFCC based on the Van Genuchten (1980) model, this can be done by choosing proper parameters α and n as reported in Table 1 whose plot is visible in the black line of Fig. 4 on the left. Let us assume the substance initially thawed at temperature T_i and force the surface to a constant temperature of T_s. The initial conditions become: $T=+2\,^{\circ}\mathrm{C}$ ($t=0$, $z>0$) and the boundary conditions: $T=-5\,^{\circ}\mathrm{C}$ ($t>0$, $z=0$) and $T=+2\,^{\circ}\mathrm{C}$ ($t>0$, $z\rightarrow\infty$) for the top and bottom boundary, respectively. The isothermal phase change and uniform thermal characteristics in the frozen and unfrozen state, may be assumed by imposing a discontinuity on the freezing front line $z=Z(t)$: $\theta_w(z)=0$, $\theta_i(z)=1$, $\lambda(z)=\lambda_i$, $C_T(z)=\rho_i c_i$ for ($t>0$, $z<Z(t)$) and $\theta_w(z)=1$, $\theta_i(z)=0$ $\lambda(z)=\lambda_w$, $C_T(z)=\rho_w c_w$ for ($t>0$, $z\geq Z(t)$), respectively. For a complete derivation of the solution see the Appendix.

The model was tested in a domain composed of 500 nodes uniformly separated by 10 mm and with an integration time $\Delta t=10$ s. Figure 3 reports the comparison between the numerical and the analytical solutions of the soil temperature profile. The temperature evolution shows a change in the slope that coincides with the separation point between the upper thawed and the lower frozen part. Furthermore, the numerical sim-

TCD
4, 1243–1276, 2010

ulation result shows oscillations, which begin at the time of phase change and then decrease with time. In fact the numerical solution the temperature starts decreasing only once all the water in the grid cell has been frozen. Furthermore, T_l is influenced by the phase change of T_{l+1} by the release of latent heat and thus the temperature oscillation continues also in the frozen state. Therefore, oscillation amplitude is both linked to the grid size and to the time: increasing the grid size, the oscillation amplitude increases, as the mass of water to freeze increases before the temperature may decrease. The oscillations amplitude dampens with time as the freezing front moves away from z_l. The oscillations amplitude may be reduced but not eliminated, as it is embedded with the fixed-grid Eulerian method, where the freezing front may move in a discrete way and not in a continuum as in the reality.

Also McKenzie et al. (2007) have compared their model (SUTRA code) against the analytical solution. They used the Lunardini (1985) solution, different from the Neumann one as it divides the region into three zones: fully frozen (with only the residual amount of unfrozen water), "mushy" (with both ice and water) and fully thawed. Their results show a good agreement with the analytical solution, however no mention is given about the grid space and integration time used with the comparison, and no temperature-time plot is provided to verify if there are oscillations as well.

The same model has been applied using different soil types (clay, silt and sand). The hydraulic and Van Genuchten parameters of silt, clay and sand have been obtained with the Rosetta Lite program (Schaap et al., 2001) and from Cainelli et al. (2010); the parameters for pure water were chosen in order to simulate a very steep SFCC with no unfrozen water content below 0 °C. The final parameters are reported in Table 1. Figure 4 on the left reports the SFCC for pure water and the different soil types, on the right reports the simulated temperature at various depths; Fig. 5 plots the freezing front advance in time. The sand, among the soils, is the fastest to freeze due to the low porosity and the steep SFCC. It is interesting to notice the difference between silt and clay: despite a higher θ_s the advance of the freezing is higher for clay because most of its water remains unfrozen in the temperature range concerned.

TCD
4, 1243–1276, 2010

7 Model testing: experimental data

In order to test the model with water movement, a comparison was made against the measured data from Fig. 5 of Hansson et al. (2004) as done by Daanen et al. (2007). Figure 6 reports the comparison of the profile of the total water content Θ (liquid+solid). Starting from a thawed condition and a uniform water content Θ=0.33, the liquid water content decreases from above due to the increase of ice content. It is visible that the freezing of the soil sucks water from below. The increase in total water content reveals the position of the freezing front: after 12 h it is located about 40 mm from the soil surface, after 24 h at 80 mm and finally after 50 h at 140 mm. Similar to Hansson et al. (2004), the results were improved by adding an impedance factor β to decrease the hydraulic conductivity close to the freezing front. It was found that the value of β that best resembles the results is 2.

The use of the impedence factor has been debated in the literature. Newman and Wilson (1997) argue that they obtained better results excluding the impedance factor for calibrating the permeability function at and behind the freezing front. In their simulations, the ice content was computed using the permeability versus suction relationship, predicted with the Fredlund and Xing (1994) equation for unsaturated soil permeability functions. Watanabe (2008) highlights that soil water flows not only through the unfrozen area but also through the frozen area. In facts he points out that a better estimation of the hydraulic conductivity of frozen soils is needed in future, especially in dealing with the impedance factor: if β=0 a huge pressure difference between the frozen and unfrozen regions induce water flow to the freezing front, where the soil quickly reaches ice saturation so that water can no longer pass through. However, increasing β to decrease the hydraulic conductivity results in a reduced water flow and decrease of ice formation at the freezing front. Therefore the impedance factor should be described in accordance with the unfrozen liquid water content instead of the ice content.

TCD
4, 1243–1276, 2010

8 Conclusions

In this paper the description and testing of a freezing soil model with variable saturation condition was presented. The model has shown a good agreement with the analytical solution of the Neumann problem although, when dealing with phase change in pure water, it shows oscillations around the analytical solution. The amplitude of the oscillations depends on the domain discretization and thus may be reduced but not eliminated, as they are embedded with the fixed-grid Eulerian method. Despite that, they do not interfere with the global behavior of the numerical solution, and can be regarded as high frequency local noise that can be removed with a smoothing filter. The model was then applied to simulate the water flow in a freezing soil, and the results were compared to the experimental findings of Hansson et al. (2004) with good agreement, even if a relatively high sensitivity to the value of the impedance factor β of the hydraulic conductivity was found.

This algorithm can potentially be applied in more realistic configurations, with complex boundary conditions accounting for the soil-atmosphere energy exchange, and thus contribute to improve our understanding of the factors controlling the soil freezing and thawing processes in the Alpine and Arctic cryosphere. Endrizzi et al. (2010), who included this algorithm in the open-source hydrological model GEOtop (Rigon et al., 2006), represent a first trial.

Appendix A

Analytical solution of phase change

Let us suppose a semi-infinite plane composed by two regions: the frozen region (subscript 1) above, and the thawed region (subscript 2) below, separated by an interface at a depth Z which moves downward in time. The system of equations in this case

TCD
4, 1243–1276, 2010

becomes:

$$\begin{cases} v_1 = v_2 = T_m & (t>0, z=Z(t)) \\ v_2 \rightarrow T_i & (t>0, z\rightarrow\infty) \\ v_1 = T_s & (t>0, z=0) \\ \lambda_1 \frac{\partial v_1}{\partial z} - \lambda_2 \frac{\partial v_2}{\partial z} = L_f \rho_w \theta_s \frac{dZ(t)}{dt} & (t>0, z=Z(t)) \\ \frac{\partial v_1}{\partial t} = d_1 \frac{\partial^2 v_1}{\partial z^2} & (t>0, z<Z(t)) \\ \frac{\partial v_2}{\partial t} = d_2 \frac{\partial^2 v_2}{\partial z^2} & (t>0, z>Z(t)) \\ v_1 = v_2 = T_i & (t=0, z) \end{cases} \quad \text{(A1)}$$

The first and second equations in Eq. (A1) give the boundary conditions at bottom ($T=T_i$) and at the surface ($T=T_s$) of the domain, respectively (Dirichlet condition); the third and fourth equations refer to the boundary conditions at the interface between the two substances, indicating that the temperatures of the two states are equal to the temperature of phase change on the surface and that the energy derived by the difference of the heat fluxes is exploited for phase change. The fifth and sixth equations refer to the approximation of steady state conduction behavior of the temperature in the two states, where $d=\lambda_T/C_T$ is the thermal diffusivity. Finally the last equation reports the initial condition in which the whole system is set at $T=T_i$.

Eventually the analytical solution becomes:

$$\begin{cases} v_1(t,z) = T_s + \frac{T_m - T_s}{\mathrm{erf}\zeta} \cdot \mathrm{erf}\frac{z}{2\sqrt{d_1 t}} & \text{if} \quad z \le Z(t) \\ v_2(t,z) = T_i - \frac{T_i - T_m}{\mathrm{erfc}\left(\zeta\sqrt{\frac{d_1}{d_2}}\right)} \cdot \mathrm{erfc}\frac{z}{2\sqrt{d_2 t}} & \text{if} \quad z > Z(t) \end{cases} \quad \text{(A2)}$$

where ζ is the solution of the following implicit algebraic equation:

$$\frac{\exp(-\zeta^2)}{\zeta \cdot \mathrm{erf}\zeta} - \frac{\lambda_{T2}\sqrt{d_1}(T_i - T_m)}{\lambda_{T1}\sqrt{d_2}(T_m - T_s)\zeta \cdot \mathrm{erfc}\left(\zeta\sqrt{\frac{d_1}{d_2}}\right)} \exp\left(-\frac{d_1}{d_2}\zeta^2\right) = \frac{L_f \rho_w \theta_s \sqrt{\pi}}{C_{T1}(T_m - T_s)} \quad \text{(A3)}$$

TCD
4, 1243–1276, 2010

In the thawing case the frozen and thawed parts are below and above $z=Z(t)$, respectively, and the analytical solution of v_1 and v_2 becomes:

$$\begin{cases} v_1(t,z) = T_i - \dfrac{T_i - T_m}{\operatorname{erfc}\left(\zeta\sqrt{\frac{d_2}{d_1}}\right)} \cdot \operatorname{erfc}\dfrac{z}{2\sqrt{d_1 t}} & \text{if} \quad z > Z(t) \\ v_2(t,z) = T_s + \dfrac{T_m - T_s}{\operatorname{erf}\zeta} \cdot \operatorname{erf}\dfrac{z}{2\sqrt{d_2 t}} & \text{if} \quad z \le Z(t) \end{cases} \tag{A4}$$

where ζ is given by the solution of:

$$\frac{\exp(-\zeta^2)}{\zeta \cdot \operatorname{erf}\zeta} - \frac{\lambda_{T1}\sqrt{d_2}(T_i - T_m)}{\lambda_{T2}\sqrt{d_1}(T_m - T_s)\zeta \cdot \operatorname{erfc}\left(\zeta\sqrt{\frac{d_2}{d_1}}\right)} \exp\left(-\frac{d_2}{d_1}\zeta^2\right) = \frac{L_f \rho_w \theta_s \sqrt{\pi}}{C_{T2}(T_m - T_s)} \tag{A5}$$

Acknowledgements. The first author would like to thank Michael Dumbser of the Department of Civil and Environmental Engineering at the University of Trento for his precious help in the numerical part of the code.

References

Anisimov, O., Shiklomanov, N., and Nelson, E.: Variability of seasonal thaw depth in permafrost regions: A stochastic modeling approach, Ecol. Model., 153, 217–227, 2002. 1244

Brooks, R. H. and Corey, A. T.: Hydraulic properties of porous media, Hydrology paper, 3, Colorado State University, Fort Collins, 1964. 1250

Cainelli, O., Tarantino, A., Costisella, C., and Bellin, A.: Does the static water retention curve reproduce correctly subsurface water dynamics?, Submitted to Water Resour. Res., submitted, 2010. 1261, 1269

Carslaw, H. and Jaeger, J.: Conduction of Heat in Solids, Clarendon Press Oxford, 1959. 1245, 1260

Christoffersen, P. and Tulaczyk, S.: Response of subglacial sediments to basal freeze-on: 1. Theory and comparison to observations from beneath the West Antarctica Ice Sheet, J. Geophys. Res., 108, 2222, doi:10.1029/2002JB001935, 2003. 1246

TCD
4, 1243–1276, 2010

Clapp, R. B. and Hornberger, G. M.: Empirical equations for some hydraulic properties, Water Resour. Res., 14, 601–605, 1978. 1250
Crank, J. and Nicolson, P.: A practical method for numeri- cal evaluation of solutions of partial differential equations of the heat-conduction type, Advances in Computational Mathematics, 6(1), 207–226, 1996. 1257
Daanen, R., Misra, D., and Epstein, H.: Active-layer hydrology in nonsorted circle ecosystems of the Arctic Tundra, Vadose Zone J., 6, 694–704, 2007. 1246, 1262
Dall'Amico, M.: Coupled water and heat transfer in permafrost modeling, Ph.D. thesis, Institute of Civil and Environmental Engineering, Università degli Studi di Trento, Trento, available from http://eprints-phd.biblio.unitn.it/335/, 2010. 1255
Endrizzi, S., Quinton, W. L. B., Marsh, P., and Dall'Amico, M.: Investigating the energy-based runoff generation theory for organic-covered permafrost using spatially distributed modelling, to be submitted to Hydrol. Earth Syst. Sci., 2010. 1255, 1263
Farouki, O. T.: The thermal properties of soils in cold regions, Cold Reg. Sci. Technol., 5, 67–75, 1981. 1252
Fredlund, D. and Xing, A.: Equations for the soil-water characteristic curve, Can. Geotech. J., 31, 521–532, 1994. 1262
Fuchs, M., Campbell, G., and Papendick, R.: An analysis of sensible and latent heat flow in a partially frozen unsaturated soil, Soil Sci. Soc. Am. J., 42, 379–385, 1978. 1246
Gardner, W.: Some steady-state solutions of the unsaturated moisture flow equation with application to evaporation from a water table, Soil Sci., 85, 228–232, 1958. 1250
Hansson, K., Simunek, J., Mizoguchi, M., Lundin, L., and van Genuchten, M.: Water flow and heat transport in frozen soil numerical solution and freeze-thaw applications, Vadose Zone J., 3, 693–704, 2004. 1245, 1246, 1247, 1254, 1259, 1262, 1263, 1276
Harlan, R.: Analysis of coupled heat-fluid transport in partially frozen soil, Water Resour. Res., 9, 1314–1323, 1973. 1245, 1246
Jame, Y. and Norum, D.: Heat and mass transfer in a freezing unsaturated porous medium, Water Resour. Res., 16, 811–819, 1980. 1246
Johansen, O.: Thermal Conductivity of Soils, Ph.D. thesis, Norwegian Technical University, Trondheim, 1975. 1252
Kelley, C.: Solving Nonlinear Equations with Newton's Method, Society for Industrial Mathematics, 2003. 1257, 1259
Loch, J.: Thermodynamic equilibrium between ice and water in porous media, Soil Sci., 126,

TCD
4, 1243–1276, 2010

77–80, 1978. 1247
Lukyanov, V. and Golovko, M.: Calculations of the Depth of Freeze in Soils, Union of Transp. Constr., Moscow, 23, 1957, (in russian). 1245
Lunardini, V.: Heat Transfer in Cold Climates, Van Nostrand Rheinhold, New York, 1981. 1244
Lunardini, V.: Freezing of soil with phase change occurring over a nite temperature difference, in: Proceedings of the 4th offshore mechanics and arctic engineering symposium, The American Society of Mechanical Engineers, 1985. 1261
Luo, L., Robock, A., Vinnikov, K., Schlosser, C., Slater, A., Boone, A., Braden, H., Cox, P., de Rosnay, P., Dickinson, R. et al.: Effects of frozen soil on soil temperature, spring infiltration, and runoff: Results from the PILPS 2 (d) experiment at Valdai, Russia, J. Hydrometeorol., 4, 334–351, 2003. 1244
McKenzie, J., Voss, C. and Siegel, D.: Groundwater flow with energy transport and water–ice phase change: Numerical simulations, benchmarks, and application to freezing in peat bogs, Adv. Water Resour., 30, 966–983, 2007. 1246, 1261
Miller, R.: Phase equilibria and soil freezing, in Permafrost: Proceedings of the Second International Conference, Washington DC: National Academy of Science-National Research Council, vol. 287, 193–197, 1965. 1247, 1248
Mualem, Y.: A new model for predicting the hydraulic conductivity of unsaturated porous media, Water Resour. Res., 12, 513–522, 1976. 1251
Nakano, Y. and Brown, J.: Effect of a freezing zone of finite width on thermal regime of soils, Water Resour. Res., 5, 1226–1233, 1971. 1245, 1260
Newman, G. and Wilson, G.: Heat and mass transfer in unsaturated soils during freezing, Can. Geotech. J., 34, 63–70, 1997. 1246, 1262
Phukan, A.: Frozen Ground Engineering, Prentice-Hall, Englewood Cliffs, NJ, 1985. 1271
Rigon, R., Bertoldi, G., and Over, T. M.: GEOtop: a distributed hydrological model with coupled water and energy budgets, J. Hydrometeorol., 7, 371–388, 2006. 1263
Schaap, M., Leij, F., and van Genuchten, M.: Rosetta: a computer program for estimating soil hydraulic parameters with hierarchical pedotransfer functions, J. Hydrol., 251, 163–176, 2001. 1261
Shoop, S. and Bigl, S.: Moisture migration during freeze and thaw of unsaturated soils: modeling and large scale experiments, Cold Reg. Sci. Technol., 25, 33–45, 1997. 1245
Smirnova, T., Brown, J., Benjamin, S., and Kim, D.: Parameterization of cold-season processes in the MAPS land-surface scheme, J. Geophys. Res., 105, 4077–4086, 2000. 1244

TCD
4, 1243–1276, 2010

Spaans, E. and Baker, J.: The soil freezing characteristic: its measurement and similarity to the soil moisture characteristic, Soil Sci. Soc. Am. J., 60, 13–19, 1996. 1248

Tomita, H.: Analysis of spurious surface temperature at the atmosphere–land interface and a new method to solve the surface energy balance equation, J. Hydrometeorol., 10, 833–844, 2009. 1259

Van Genuchten, M. T.: A closed-form equation for predicting the hydraulic conductivity of unsaturated soils., Soil Sci. Soc. Am. J., 44, 892–898, 1980. 1250, 1260, 1270

Viterbo, P., Beljaars, A., Mahfouf, J., and Teixeira, J.: The representation of soil moisture freezing and its impact on the stable boundary layer, Q. J. Roy. Meteor. Soc., 125, 2401–2426, 1999. 1244

Watanabe, K.: Water and heat flow in a directionally frozen silty soil, Proceedings of the third HYDRUS Workshop, Jun 28, 2008, Tokyo University of Agriculture and Technology, Tokyo, Japan, ISBN:978-4-9901192, 15–22, 2008. 1247, 1262

Williams, P. and Smith, M.: The Frozen Earth: Fundamentals of Geocryology, Cambridge University Press, 1989. 1245, 1254

Zhang, X., Sun, S., and Xue, Y.: Development and testing of a frozen soil parameterization for cold region studies, J. Hydrometeorol., 8, 690–701, 2007. 1249

Zhang, Y., Carey, S., and Quinton, W.: Evaluation of the algorithms and parameterizations for ground thawing and freezing simulation in permafrost regions, J. Geophys. Res, 113, D17116, doi:10.1029/2007JD009343, 2008. 1244, 1245

TCD
4, 1243–1276, 2010

Table 1. Porosity and Van Genuchten parameters for water and different soil types.

	θ_s (–)	θ_r (–)	α (mm^{-1})	n (–)	Source
Water	1.0	0.0	4E-1	2.50	
Sand	0.3	0.0	4.06E-3	2.03	Cainelli et al. (2010)
Silt	0.489	0.05	6.5E-4	1.67	Rosetta Lite
Clay	0.459	0.098	1.49E-3	1.25	Rosetta Lite

TCD
4, 1243–1276, 2010

Table A1. Table of symbols used.

Symbol	Name	Value or Range	Unit
t	time		s
T	temperature		°C
ρ_w	density of liquid water in soil	1000	kg m^{-3}
ρ_i	density of ice	918	kg m^{-3}
θ_i	fraction of ice in soil		dimensionless
θ_w	fraction of liquid water in soil		dimensionless
z_f	elevation with respect to a reference		m
g	gravity acceleration	9.81	m s^2
$\Delta\theta_w^{ph}$	variation of liquid water due to phase change		dimensionless
$\Delta\theta^{ph}$	variation of ice due to phase change		dimensionless
$\Delta\theta_w^{h}$	variation of liquid water due to fluxes		dimensionless
ω	explicit-implicit parameter		dimensionless
V_c	volume of control in the soil		m^3
Ω	cell area		m^2
β	impedance factor		dimentionless
θ_s	soil porosity		dimensionless
θ_r	residual water content		dimensionless
Θ	total water (liquid and ice) content in soil		dimensionless
ψ_{w0}	soil pressure head corresponding to total water content		m
p_a	reference atmospheric pressure		Pa
ψ	soil water pressure head		m
T_m	water freezing temperature at atmospheric pressure	273.15	K
T^*	depressed water freezing temperature in the soil		K
α	SWCC parameter (Van Genuchten, 1980)		mm^{-1}
n	SWCC parameter (Van Genuchten, 1980)		dimensionless
$\boldsymbol{J}_w$	volumetric liquid water flux		m s^{-1}
$\boldsymbol{J}_i$	volumetric ice flux		m s^{-1}
K_H	hydraulic conductivity		m s^{-1}
λ_T	total thermal conductivity of soil		W m^{-1} K^{-1}
λ_w	water thermal conductivity	0.6	W m^{-1} K^{-1}
λ_i	ice thermal conductivity	2.29	W m^{-1} K^{-1}
d_w	water thermal diffusivity	1.43E-7	m^2 s^{-1}
d_i	ice thermal diffusivity	1.13E-6	m^2 s^{-1}
L_f	latent heat of fusion	333.7	kJ kg^{-1}
$C_H[\psi(T)]$	hydraulic capacity of soil		m^{-1}
$C_T(T)$	total volumetric thermal capacity of soil		J m^{-3} K^{-1}
C_{sp}	volumetric thermal capacity of soil particles		J m^{-3} K^{-1}
$C_a(T)$	volumetric apparent thermal capacity of soil		J m^{-3} K^{-1}
c_i	specific thermal capacity of ice	2117	J kg^{-1} K^{-1}
c_w	specific thermal capacity of water	4188	J kg^{-1} K^{-1}
U	volumetric internal energy of soil		J m^{-3}
S_{en}	sink term of energy losses		W m^{-3}
S_w	sink term of mass losses		s^{-1}
$\boldsymbol{G}$	heat conduction flux in the ground		W m^{-2}
$\boldsymbol{J}$	heat flux due to water advection		W m^{-2}
H	Heaviside function		dimensionless

TCD
4, 1243–1276, 2010

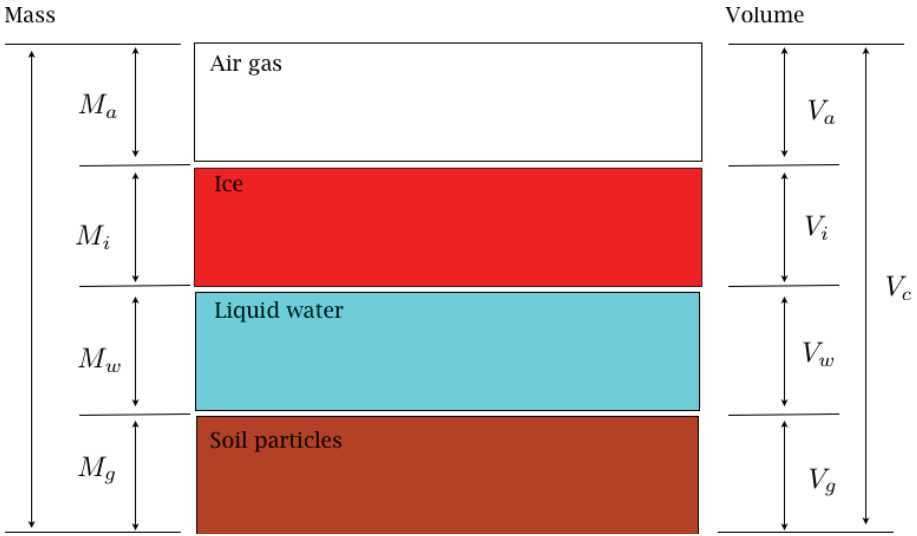

Fig. 1. Frozen soil constituents and schematization of the control volume V_c after Phukan (1985).

TCD
4, 1243–1276, 2010

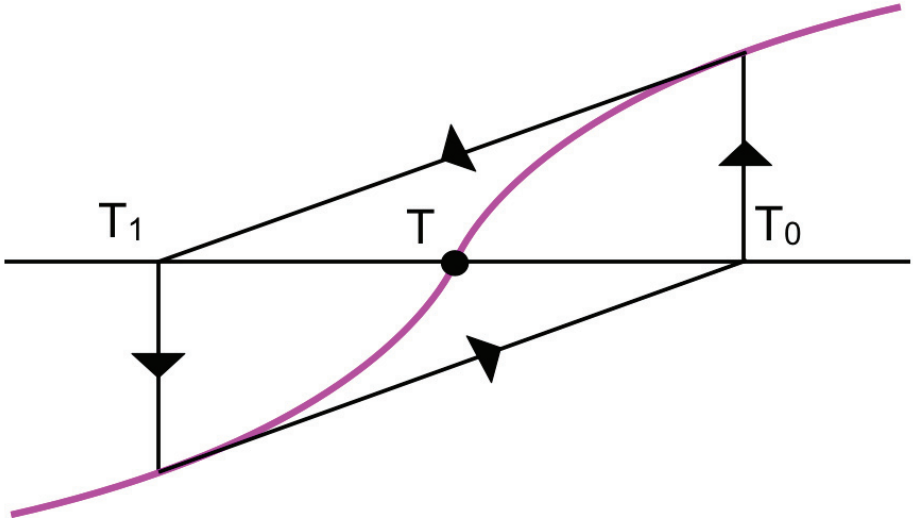

Fig. 2. Schematization of a non convergent Newton-Raphson method.

TCD
4, 1243–1276, 2010

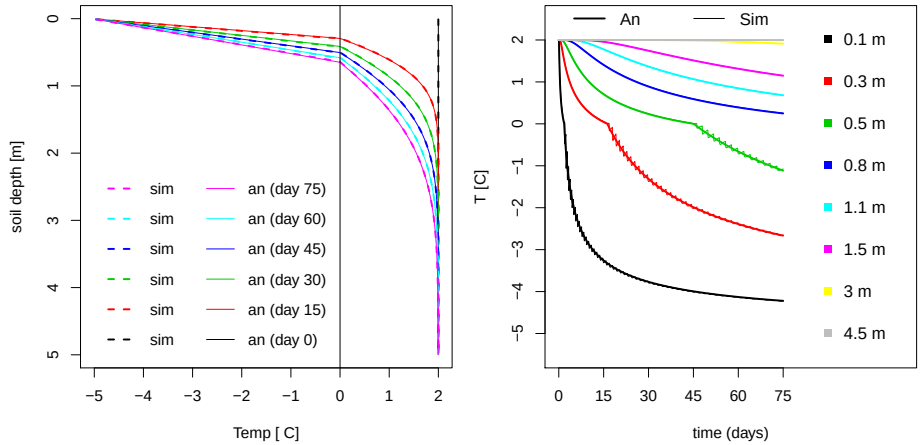

Fig. 3. Comparison between the simulated numerical and the analytical solution. Left: soil profile temperature at different time frames. Right: temperature behavior in time at different depths. Grid size=10 mm, N=500 points.

TCD
4, 1243–1276, 2010

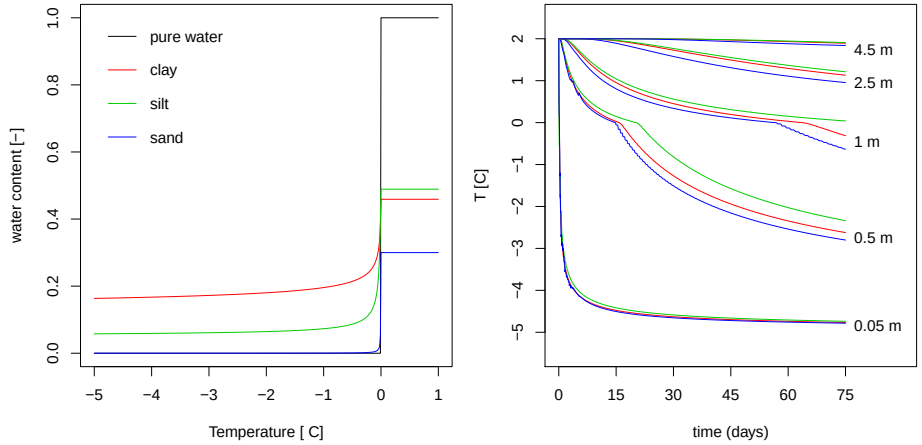

Fig. 4. Left: soil freezing curve for pure water and various soil textures, according to proper Van Genuchten parameters. Right: freezing of different soil types.

TCD
4, 1243–1276, 2010

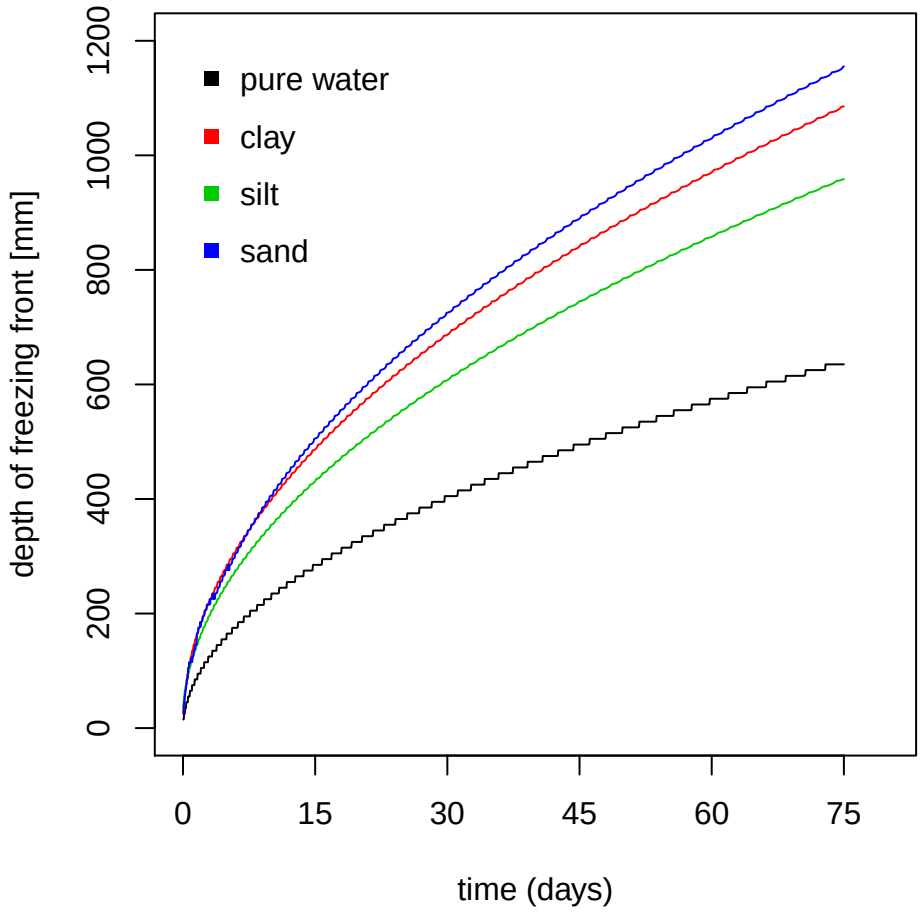

Fig. 5. Freezing front (mm) advancing in time for pure water and different soil types.

TCD
4, 1243–1276, 2010

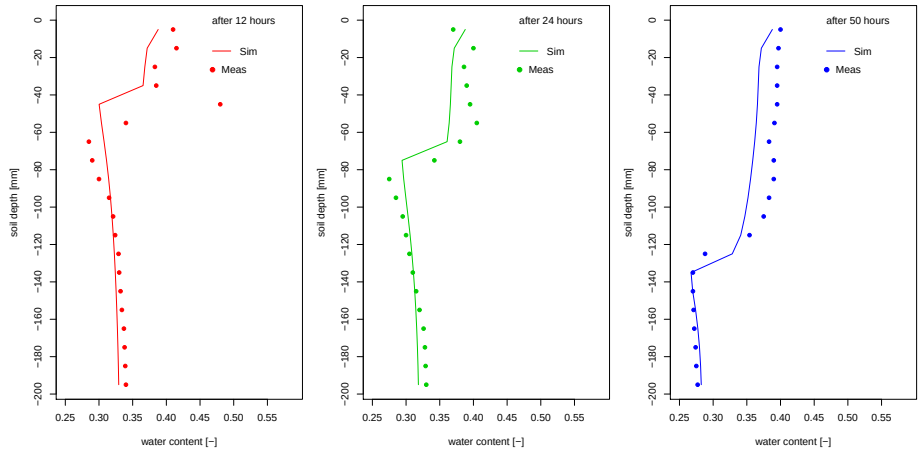

Fig. 6. Comparison between the numerical (plain line) and the experimental results (points) obtained by Hansson et al. (2004) of the total water (liquid plus ice) after 12 h.

TCD
4, 1243–1276, 2010